This paper is available on line at http://www.mcponline.org

TvMP50 is an Immunogenic Metalloproteinase during Male Trichomoniasis*[S]

Laura Itzel Quintas-Granados‡, José Luis Villalpando‡, Laura Isabel Vázquez-Carrillo‡, Rossana Arroyo§, Guillermo Mendoza-Hernández¶, and María Elizbeth Álvarez-Sánchez‡‖

Trichomonas vaginalis*, a human urogenital tract parasite, is capable of surviving in the male microenvironment, despite of the presence of Zn^{2+}. Concentrations > 1.6 mM of Zn^{2+} have a trichomonacidal effect; however, in the presence of ≤1.6 mM Zn^{2+}, several trichomonad proteins are up- or down-regulated. Herein, we analyzed the proteome of a *T. vaginalis* male isolate (HGMN01) grown in the presence of Zn^{2+} and found 32 protein spots that were immunorecognized by male trichomoniasis patient serum. Using mass spectrometry (MS), the proteins were identified and compared with 23 spots that were immunorecognized in the proteome of a female isolate using the same serum. Interestingly, we found a 50-kDa metallopeptidase (TvMP50). Unexpectedly, this proteinase was immunodetected by the serum of male trichomoniasis patients but not by the female patient serum or sera from healthy men and women. We analyzed the *T. vaginalis* genome and localized the *mp50* gene in locus TVAG_403460. Using an RT-PCR assay, we amplified a 1320-bp *mp50* mRNA transcript that was expressed in the presence of Zn^{2+} in the HGMN01 and CNCD147 *T. vaginalis* isolates. According to a Western blot assay, native TvMP50 was differentially expressed in the presence of Zn^{2+}. The TvMP50 proteolytic activity increased in the presence of Zn^{2+} in both isolates and was inhibited by EDTA but not by *p*tosyl-L-lysine chloromethyl ketone (TLCK), E64, leupeptin, or phenylmethane sulfonyl fluoride. Furthermore, the recombinant TvMP50 had proteolytic activity that was inhibited by EDTA. These data suggested that TvMP50 is immunogenic during male trichomoniasis, and Zn^{2+} induces its expression. *Molecular & Cellular Proteomics 12: 10.1074/mcp.M 112.022012, 1953–1964, 2013.

Trichomoniasis is the most common nonviral sexually transmitted infection. The infection is caused by *Trichomonas vaginalis* with ~174 million new cases per year worldwide (1). This infection is implicated as a cofactor in the transmission of the human immunodeficiency virus (2). Infected women develop vaginitis, cervicitis, urethritis, and malodourous seropurulent vaginal discharge with serious health consequences such as infertility (3–4), preterm delivery, low-birth weight infants (5), and a predisposition to cervical neoplasia (6). In men, the infection is mainly asymptomatic (7) and self-limiting, although there are complications such as urethritis, prostatitis, and an association with prostate cancer and infertility (8–11).

The primary antimicrobial defenses of the male genitourinary tract are prostatic and seminal fluids with high levels of Zn^{2+} (4.5 to 7 mM) (12). In particular, Zn^{2+} is the major prostate defense due to its ability to prevent pathogens from establishing in the reproductive male tract (12). Indeed, it has an antimicrobial spectrum that includes bacteria, viruses, chlamydiae and fungi (13). *T. vaginalis* is sensitive to relatively low concentrations of Zn^{2+} and has a minimum trichomonacidal concentration of 1.6 mM (12). However, the Zn^{2+} concentration (~0.8 mM) found in patients with chronic bacterial prostatitis is not trichomonacidal (14) and *T. vaginalis* may persist for longer periods of time in the male genitourinary tract. Parasites may possibly progress to the prostate, where they have been observed to infect the prostatic epithelium causing chronic prostatitis and elicit an inflammatory immune response (15). Indeed, *T. vaginalis* has been observed in prostate tissue near inflammation areas and epithelial hyperplasia, suggesting that this parasite might be involved in prostate carcinogenesis (9).

Recently, we reported that the variation in trichomonal pathogenesis between the sexes might imply different host-parasite molecular interactions and changes in the parasite proteome (16). At least five trichomonad proteinases (CP70, TvCP65, CP39, CP25, and CP20) are involved in the interaction between parasites and prostatic DU-145 cells. Interestingly, the trichomonal cytotoxicity toward DU-145 cells is 80% lower than it is in HeLa cells. Furthermore, parasites display an oval form and pseudopods forming upon contact with DU-145 cells, but amoeboid trophozoites were not observed (16). Interestingly, proteolytic activity and the amount of TvCP65, a cysteine proteinase involved in trichomonal cytotoxicity toward cervical cells (17–18) and its transcript are

From the ‡Posgrado en Ciencias Genómicas, Universidad Autónoma de la Ciudad de México (UACM), San Lorenzo # 290, Col. Del Valle, CP 03100. México D.F., México; §Departamento de Infectómica y Patogénesis Molecular, Centro de Investigación y de Estudios Avanzados del IPN (CINVESTAV-IPN), Av IPN 2508, Col. San Pedro Zacatenco CP 07360. México D.F., México; ¶Departamento de Bioquímica, Facultad de Medicina, Universidad Nacional Autónoma de México, México, D.F., México

Received July 10, 2012, and in revised form, March 21, 2013
Published, MCP Papers in Press, DOI 10.1074/mcp.M112.022012

diminished by 80% in the presence of Zn^{2+}(16). In a previous study, we identified a 50-kDa metalloproteinase that was highly expressed in the presence of Zn^{2+} in the CNCD147 female isolate (16).

This work examines the immunoproteome of the *T. vaginalis* HGMN01 male isolate compared with the CNCD147 female isolate. This work also reports on the characterization of a metalloproteinase that is differentially immunodetected by male trichomoniasis serum in the presence of Zn^{2+}. This difference could be a starting point for the diagnosis of this infection.

EXPERIMENTAL PROCEDURES

T. vaginalis Culture—Trophozoites of *T. vaginalis* isolate CNCD147 (female) or HGMN01 (male) were axenically cultivated for 24 h in trypticase-yeast extract-maltose (TYM) medium, pH 6.2, with 10% heat-inactivated horse serum (Invitrogen) and supplemented with or without 1.6 mM $ZnCl_2$ (Sigma).

RNA Extraction and cDNA Synthesis—For RNA extraction, we used 2×10^7 parasites from both *T. vaginalis* isolates grown with or without 1.6 mM of Zn^{2+} and treated as previously described (19). Briefly, 1 μg of total RNA was reverse-transcribed using the Superscript Reverse Transcriptase Kit (Invitrogen, Carlsbad, CA) and an oligo-dT (dT18) (10 pmol/μl) primer. The cDNA obtained was stored at −20 °C until use.

Analysis of mp50 mRNA Expression by Semiquantitative RT-PCR—PCR was performed in 50 μl reactions containing 50 ng of cDNA, as previously reported (16). We used the following primer pairs to amplify the 1320-bp *mp50* gene: forward, 5′- CC*GGATCC*ATGTCAGGTGAC-GAATTC-3′ (BamHI recognition site is underlined) and reverse, 5′-CC*AAGCTT*TCAAAGTACTCTTGAAGC-3′ (HindIII recognition site underlined). In addition, a 112-bp fragment of the *β-tubulin* gene was used as a loading control (20). The amplified products were analyzed on 1% agarose gels and visualized by ethidium bromide staining. Gene expression densitometry analyses were performed with Quantity One Software (Bio-Rad, Hercules, CA). Data from the densitometry quantification of the housekeeping gene (*β-tubulin*) were used to normalize the results.

Two-dimensional Electrophoresis—For proteomic maps, we used a previously reported protocol (16) with modifications (for details see the supplemental experimental procedures in the Supplemental Data file). Briefly, 70 μg of protein was applied to an IPG strip (17 cm, pH 4–7 linear; Bio-Rad) for passive rehydration for 12 h. Then, the equilibrated IPG strips were separated in 12% SDS-PAGE gels (20 cm × 20 cm × 1.0 mm) and stained with SYPRO® Ruby Protein Gel Stain (Invitrogen), following procedures described by the manufacturer. Finally, the gels were documented using Gel Doc EQ (Bio-Rad) system. Image analysis was performed using PDQuest software (Bio-Rad). Three independent protein preparations, each obtained from an independent parasite culture, were performed for comparisons of the two-dimensional electrophoresis (2DE)[1] maps.

Human Biological Samples—The serum samples from trichomoniasis patients were donated by Rossana Arroyo PhD, obtained as previously reported (21). The serum samples were obtained from trichomoniasis patients attending the "Centro Nacional de Clinicas de Displasias (CNCD)" and "Laboratorio Central" from the "Hospital General de Mexico" (HGM) at Mexico City. All patients agreed to participate in this study via written informed consent and the study was approved by the Bioethics Standard Committee (21). In this discovery stage study, either male (HGMN01) or female (HGM124) sera were used (22). Healthy sera from males and females were used as negative controls (for details see the supplemental experimental procedures in the Supplemental Data file).

Immunoblot Analysis of Two-dimensional Electrophoresis—The 2DE-PAGE separated proteins were electroblotted onto nitrocellulose membranes (GE Healthcare, USA) as previously reported (23). After being blocked, the membranes were incubated with a 1:500 dilution of HGMN01 or HGM124 serum from trichomoniasis patients at 4 °C overnight. Next, the membranes were further incubated with a 1:3000 dilution of peroxidase-labeled rabbit anti-human IgG (Jackson Immunoresearch Laboratories, West Grove, PA) for 1 h at room temperature and developed using an enhanced chemiluminescence ECL Plus Western blotting Detection System (GE Healthcare), according to the manufacturer's instructions (for details see the supplemental experimental procedures in the Supplemental Data file).

Liquid Chromatography Electrospray Ionization Quadrupole Time of Flight Mass Spectrometry—The MS analysis of each fraction obtained from the offline separation steps was conducted according to a previously reported method (16) (for details see the supplemental experimental procedures in the Supplemental Data file).

Data Processing and Search Parameters—Peaklists were generated using Mascot Distiller v2.1. For MS/MS data analysis, the MASCOT server (Matrix Science, London, UK, available at http://www.matrixscience.com, version 2.2; Matrix Science, London, UK) was used to search against the NCBI database nr 2011.07.09 (14652852 sequences, 5012444178 residues). The default search parameters were such that a Mascot threshold score of 5% indicated that the protein identification was likely incorrect. All samples were searched with the taxonomy filter "Other Eukaryota" (379307 sequences).The database search parameters were set as follows: enzyme (trypsin with a maximum of one missed cleavages); fixed modifications (carbamidomethyl (+57.021 Da at cysteine residue)); variable modifications (deamidated (+1 Da at cysteine residue)) and methionine oxidation (+15.995 Da at methionine residue); peptide mass tolerance (± 1.2 Da); fragment mass tolerance (± 0.6 Da); mass tolerance for precursor ions (100 ppm); and mass tolerance for fragment ions (0.6 Da). The protein identification reporting criteria included at least two MS/MS spectrum matched at the 95% level of confidence (Mowse score = 25) and the presence of a consecutive γ and/or β ion series of three or more amino acids.

The functional classification of the *T. vaginalis* immunoproteome was performed according to the Gene Ontology index (http://www.geneontology.org/).

Proteolytic Activity of Native TvMP50—A proteinase extract was obtained as previously reported (17). The supernatant was loaded into Bio-gel P6 Micro Bio-Spin chromatography columns (Bio-Rad) and eluted in 10 mM Tris-HCl, pH 7.5, according to the manufacturer's instructions (for details see the supplemental experimental procedures in the Supplemental Data file). Metallopeptidase activity was analyzed by one- or two-dimensional gelatin zymography under non-reducing conditions, using 10% SDS-PAGE copolymerized with 0.2% gelatin as previously reported (24). The cysteine peptidase activity was also tested under reducing conditions as previously described (17). The gels were stained with 0.25% Coomassie Brilliant Blue with clear bands against a black background corresponding to zones of digestion.

Samples containing 20 μg of proteinase extract were incubated at 4 °C for 20 min in the presence or absence of several proteinase

[1] The abbreviations used are: 2DE, two dimensional electrophoresis; 2DE-WB, 2DE immunoblot analysis; TLCK, *p*tosyl-L-lysine chloromethyl ketone; E64, L-3-carboxy-2,3-*trans*-epoxypropionyl-leucylamido(4-guanidino)butane; PMSF, phenylmethane sulfonyl fluoride; LC-ESI-QUAD-TOF, Liquid Chromatography Electrospray Ionization Quadrupole Time of flight.

inhibitors 0.25 mM E64, 1.0 mM *p*tosyl-L-lysine chloromethyl ketone (TLCK) and 1.0 mM leupeptin for cysteine proteinases, 1.0 mM phenylmethane sulfonyl fluoride (PMSF) for serine proteinases and 0.2 mM EDTA for metalloproteinase (all purchased from Sigma Chemical Co) and analyzed as described above.

Expression, Purification, and Proteolytic Activity of Recombinant TvMP50—The 1320-bp *mp50* gene was digested using BamHI and HindIII (both from New England BioLabs, Ipswitch, MA) and ligated with T4 DNA ligase into the pQE80L expression vector (Qiagen, Valencia, CA) according to the manufacturer's instructions. Positive recombinant clones were identified by sequencing (3130 Genetic Analyzer, Applied Biosystems, Foster City, CA). The recombinant TvMP50 (rTvMP50) was expressed using the M15 *E. coli* strain by adding 1 mM IPTG (isopropyl-1-thio-β-D-galactopyranoside). Purification of 6xHis-tagged rTvMP50 was performed by nickel affinity chromatography according to the manufacturer's instructions using a 1-ml HisTRap HP precast column (GE Healthcare) under native conditions. The identity of rTvMP50 was corroborated by Western blot analysis using an anti-His-Tag antibody as previously described (25). Anti-rTvMP50 polyclonal antibody was obtained using a standard protocol (for details see the supplemental experimental procedures in the Supplemental Data file). Anti-rTvMP50 was used to perform Western blot analysis with the *T. vaginalis* total protein extract from HGMN01 and CNCD147 isolates grown in the presence or absence of Zn^{2+} obtained by TCA precipitation as previously reported (17) (for details see the supplemental experimental procedures in the Supplemental Data file). The proteolytic activity of rTvMP50 was evaluated as described above.

RESULTS

Immunoproteome of T. vaginalis Isolates HGMN01 and CNCD147—The proteomic analyses were performed using two *T. vaginalis* isolates, CNCD147 and HGMN01 from an infected woman and man, respectively.

For the comparative proteomic analysis, images of three representative 2-DE gels obtained from three independent experiments using parasites grown in the presence and absence of 1.6 mM Zn^{2+} from the different isolates were analyzed with PDQuest software (data not shown). The proteomic profiles from either the *T. vaginalis* HGMN01 or CNCD147 isolates were highly reproducible in terms of the total number of protein spots and their relative positions and intensities. SYPRO® Ruby-stained gels from the *T. vaginalis* HGMN01 isolate displayed ~609 spots in the control (absence of Zn^{2+})(Fig. 1*A*), whereas 540 spots were obtained in the presence of Zn^{2+} (Fig. 1*C*). In contrast, the CNCD147 isolate displayed 447 (Fig. 2*A*) spots in the control, whereas 361 spots were observed in the presence of Zn^{2+} (Fig. 2*C*). Proteins detected in pI range of 4–7 had molecular masses between 10 and 250 kDa. The gels displayed remarkable changes in protein profiles when parasites were grown in the presence of Zn^{2+}. In addition, duplicate of these gels were transferred onto nitrocellulose membranes for Western blot analyses using serum from a male trichomoniasis patient (Figs. 1*B* and 1*D* and Figs. 2*B* and 2*D*).

Interestingly, 52 spots were immunodetected in the HGMN01 isolate using the male patient serum and the control parasites (Fig. 1*B*), whereas 32 spots were detected in the total protein extract from parasites grown in the presence of Zn^{2+} (Fig. 1*D*). Moreover, this serum immunodetected 29 spots from the control parasites of the CNCD147 isolate (Fig. 2*B*) and 23 spots from parasites grown in the presence of Zn^{2+} (Fig. 2*D*). These spots were identified by LC-ESI-QUAD-TOF. The accession numbers, protein scores, theoretical and experimental pI and molecular weights and sequence coverage of all identified proteins in the *T. vaginalis* male immunoproteome are shown in supplemental Tables S1 to S3. (For specific details of Peptide Mass Fingerprint (PMF) see Supplemental Tables I to VI).

The proteins identified in our immunoproteome discovery study are mostly hypothetical, cytoskeleton proteins and proteins involved in glycolysis and carbohydrate metabolism (supplemental Fig. S1 in Supplemental Data file). Interestingly, proteins involved in redox homeostasis, fermentative metabolism, adhesion, protein synthesis, and amino acid catabolism were immunogenic. Proteins from secretion pathways, phagocytosis, ATP synthesis, chaperons, and heat shock proteins were less abundant but also immunogenic. Furthermore, putative cysteine and metalloproteinases were identified as immunogenic molecules.

Surprisingly, protein spots 6 and 66, which corresponded to the same aminopeptidase P-like metallopeptidase from Clan MG and family M24 (supplemental Table S1), were overexpressed in the presence of Zn^{2+} in the two isolates according to 3D view analysis using the Melanie software (Figs. 1*E* and 2*E*, panels b and h). Interestingly, in the presence of Zn^{2+}, only the spot corresponding to TvMP50 was found in both isolates (supplemental Fig. S2 in the Supplemental Data file). In contrast, in the absence of this cation, we found no overlapping proteins (Supplemental Fig. S2 in Supplemental Data file).

Interestingly, in a comparative analysis of the close-ups of these spots, immunodetection by the male trichomoniasis patient serum (Figs. 1*E*, panels c, i and 2*E*, panel i) but not by the female patient serum (Figs. 1*E* and 2*E*, panels d and j) or by the healthy male or female people serum (Figs. 1*E* and 2*E*, panels e, f, k and l) was observed. Unexpectedly, this metallopeptidase was undetectable in the CNCD147 isolate in the control trichomonads. This observation correlated with the fact that this molecule was not detected by the female patient serum.

T. vaginalis Contains a 50-kDa Metallopeptidase Gene Differentially Expressed in the Presence of Zn^{2+}—We found that the immunogenic aminopeptidase P-like metalloproteinase is encoded by a 1320-bp ORF termed *mp50* (GenBank accession number JF263458), located in the locus TVAG_403460 (supplemental Fig. S3 in Supplemental Data file), which contains another two ORFs on the opposite strand that encode a calcium-dependent lipid-binding protein and a conserved hypothetical protein (supplemental Fig. S3 in the Supplemental Data file). The *mp50* gene encodes a 439-amino acid protein with a predicted molecular weight of 50,416 Da.

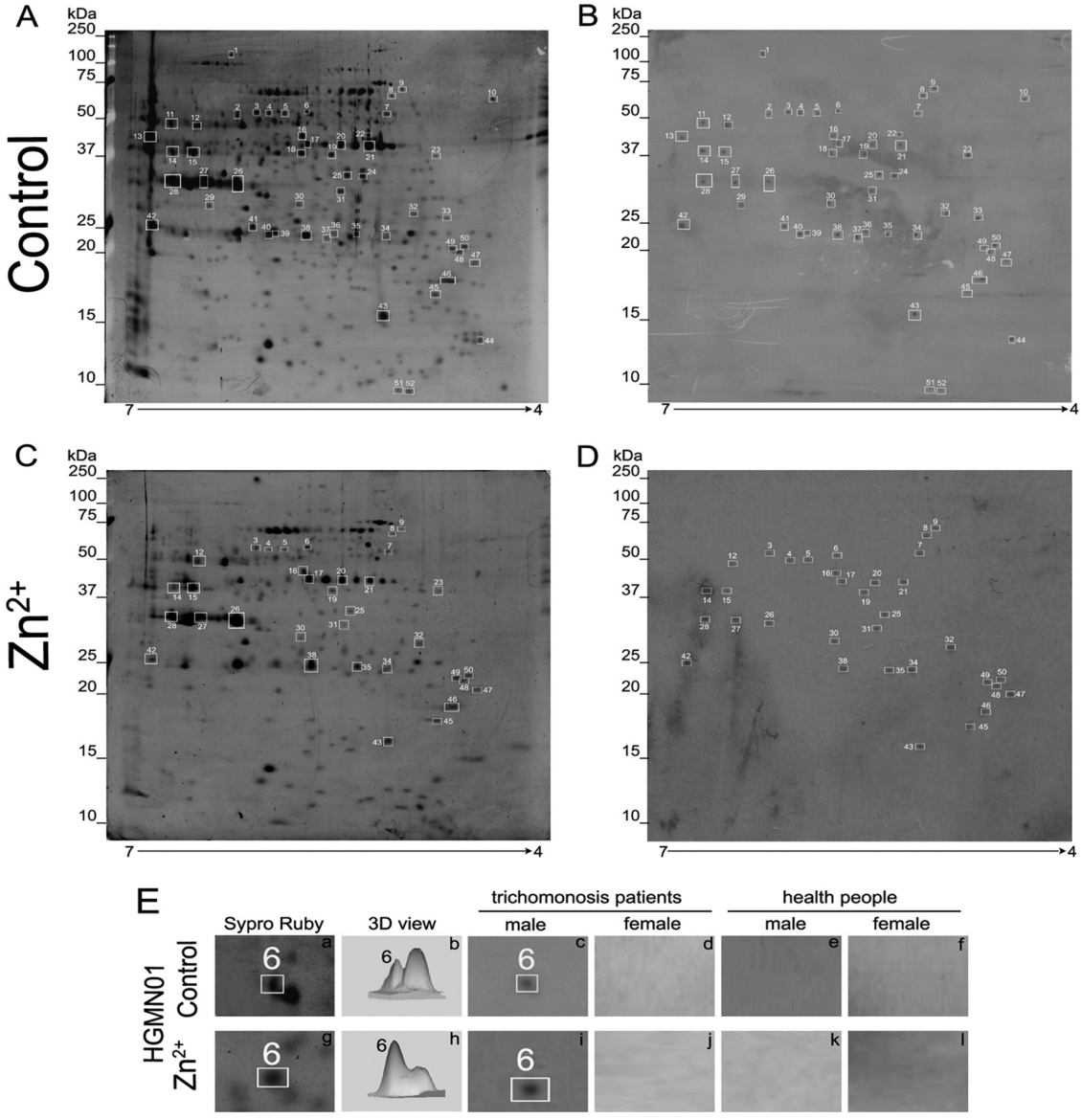

FIG. 1. **Zn^{2+} proteomic map of *T. vaginalis* isolate HGMN01**. The total proteins of *T. vaginalis* grown in the absence (*A* and *B*) or the presence (*C* and *D*) of 1.6 mM Zn^{2+} were separated in the first dimension by isoelectric focusing over a pH range from 4.0 to 7.0 followed by 12% SDS-polyacrylamide gel electrophoresis (*A* and *C*) or transferred to a nitrocellulose membrane for Western blot analysis using serum from a trichomoniasis male patient (*B* and *D*). The spots immunodetected by the serum from a male trichomoniasis patient are indicated with squares. *E*, HGMN01 isolate cultivated in the absence (control) (panels a–f) or presence of Zn^{+2} (panels g–l). Close-up of the 50-kDa metalloproteinase region of the 2 DE gels (panels a and g), 3D view of spots in panel a or panel g (panels b and h, respectively) and 2DE-WB (panels c–f and i–l) using male (panels c and i) or female (panels d and j) trichomoniasis patients sera and male (panels e and k) or female (panels f and l) healthy people sera. The white squares show spot 6, which corresponds with the Zn^{2+}-differential expressed TvMP50 in the HGMN01 isolate (panel g and h) and the TvMP50 immunorecognition by male sera with trichomoniasis (panels c and i).

The deduced amino acid sequence of TvMP50 was aligned with metallopeptidases representative of subfamilies A (data not shown) and B (supplemental Fig. S3 in Supplemental Data file) from family M24 of clan MG. The primary structure of TvMP50 is highly conserved at the amino acid residues that interact with the metal ion and the residues from the catalytic site when compared with the subfamily B peptidases. In this clan, three histidine residues form the catalytic triad. Interestingly, TvMP50 contains these catalytic residues located in similar positions. Both the amino acid residues that bind to the metal ion in this clan (D, D, H, E) and also the amino acids surrounding the metal-binding residues are conserved in TvMP50, suggesting that this molecule might be a member of this clan.

According to RT-PCR semiquantitative analyses, *mp50* mRNA displayed a differential expression level in the presence of Zn^{2+} in both the CNCD147 and HGMN01 *T. vaginalis* isolates (Fig. 3*A*). In the CNCD147 isolate, the *mp50*

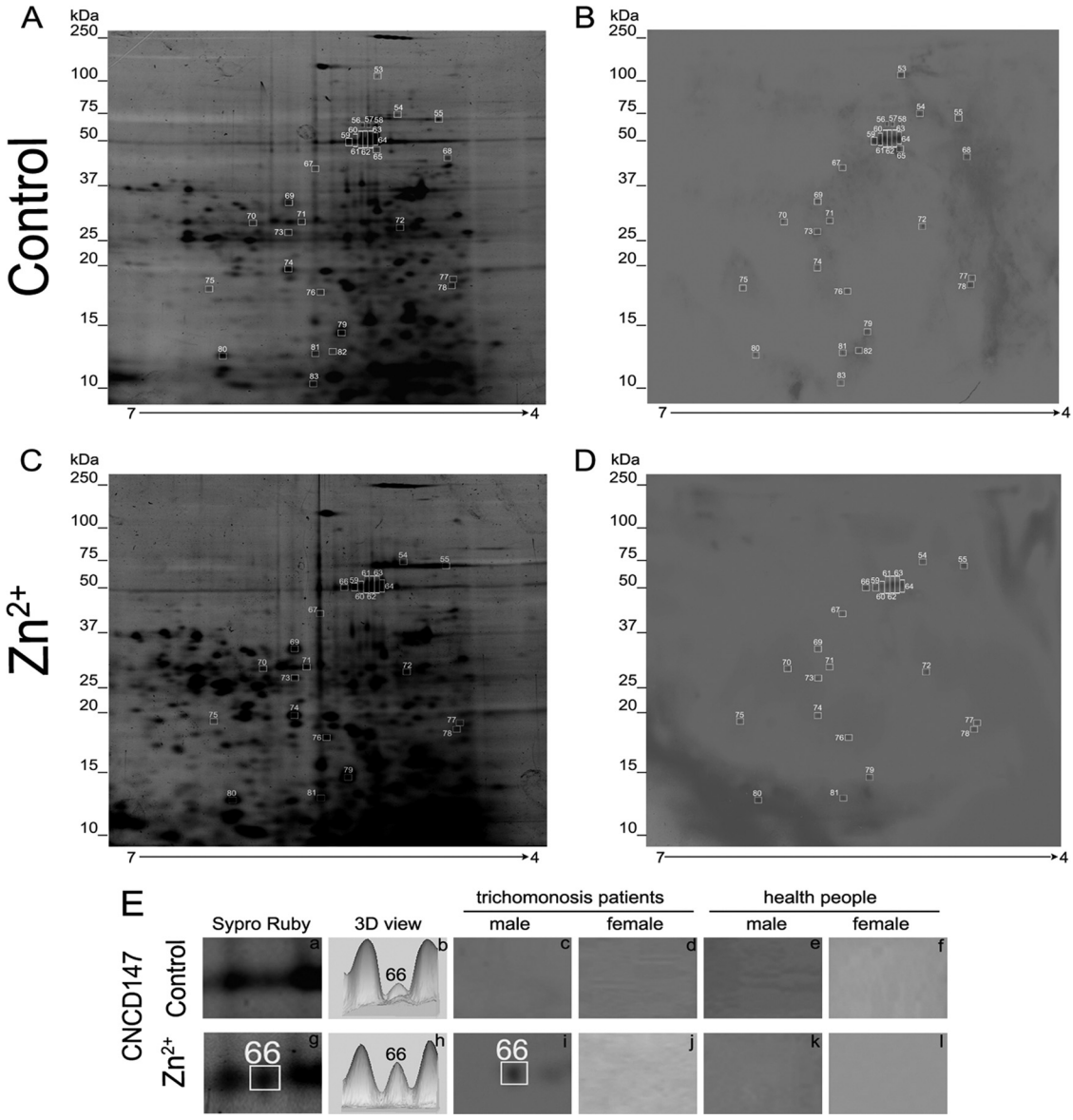

FIG. 2. **Zn^{2+} proteomic map of *T. vaginalis* isolate CNCD147**. The total proteins of *T. vaginalis* grown in the absence (*A* and *B*) or the presence (*C* and *D*) of 1.6 mM Zn^{2+} were separated in the first dimension by isoelectric focusing over a pH range from 4.0 to 7.0 followed by 12% SDS-polyacrylamide gel electrophoresis (*A* and *C*) or transferred to a nitrocellulose membrane for Western blot analysis using serum from a trichomoniasis male patient (*B* and *D*). The spots immunodetected by the serum from a male trichomoniasis patient are indicated with squares. *E*, CNCD147 isolate cultivated in the absence (control) (panels a–f) or presence of Zn^{+2} (panels g–l). Close-up of the 50-kDa metalloproteinase region of the 2DE gels (panels a and g), 3D view of spots in panel a or panel g (panels b and h, respectively) and 2DE-WB (panels c–f and i–l) using male (panels c and i) or female (panels d and j) trichomoniasis patient sera and male (panels e and k) or female (panels f and l) healthy people sera. The white squares show spot 66, which corresponds with Zn^{2+}-differential expressed TvMP50 in the CNCD147 isolate (panel g and h) and the TvMP50 immunorecognition by male trichomoniasis patient sera with (panel i).

mRNA was almost undetectable (Fig. 3*A*, mp50, lane 1) in the absence of Zn^{2+}. However, in the presence of Zn^{2+}, *mp50* mRNA expression was detected (Fig. 3*A*, mp50, lane 2). Moreover, in the HGMN01 isolate, the *mp50* transcript was detected even in the absence of Zn^{2+} (Fig. 3*A*, mp50, lane 3); however, its expression increased in the presence of this cation (Fig. 3*A*, mp50, lane 4). In contrast, no differences were found in the expression of the β *tubulin* transcript used as a loading control (Fig. 3*A*, β tub). The normalized intensity of the bands used for densitometric analyses indicated that in the presence of Zn^{2+} and a 100% *mp50* mRNA level was found in the female isolate (CNDC147) (supplemental Fig. S4 in the Supplemental Data file), whereas a 50% *mp50* mRNA level was found in the male isolate (HGMN01), confirming the differential expression of the *mp50* transcript.

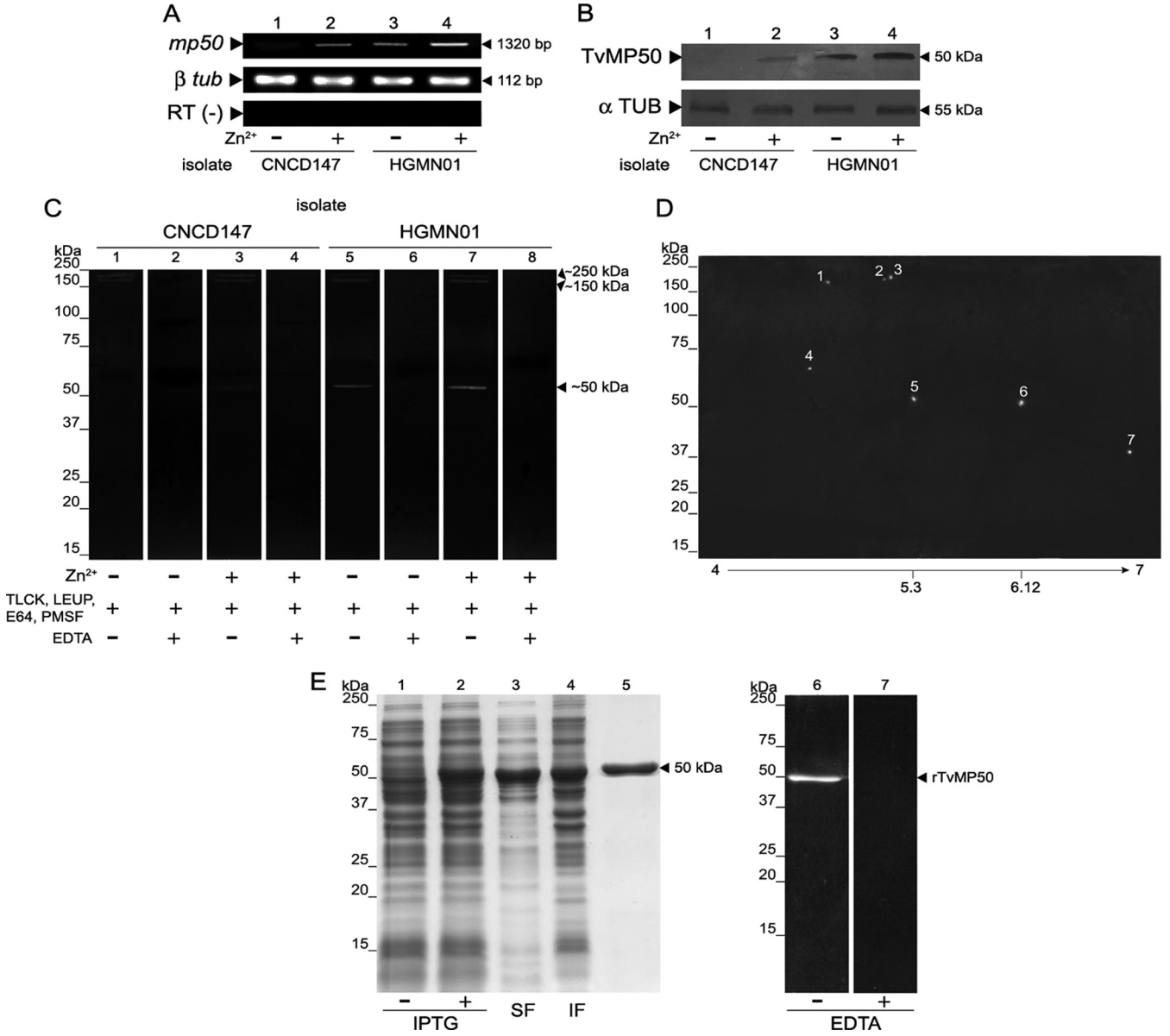

FIG. 3. **Zn^{2+} effect on the *mp50* transcript, native TvMP50 and its proteolytic activity.** *A*, Semi-quantitative RT-PCR analyses to detect the 1320-bp *mp50* or 112-bp *β-tubulin* transcript using cDNA from parasites of CNCD147 (lanes 1 and 2) or HGMN01 (lanes 3 and 4) isolates, cultivated in the absence (lanes 1 and 3) or presence 1.6 mM (lane 2 and 4) of Zn^{2+} and RT(−), as a negative control. Arrowheads indicate the 1320-bp and 112-bp RT-PCR products for the *mp50* and *β-tubulin* transcripts, respectively. These experiments were performed at least three times with similar results. *B*, Western blot analysis to detect the native TvMP50. TCA-total protein extracts obtained from CNCD147 (lanes 1 and 2) or HGMN01 (lanes 3 and 4) isolates cultivated in the absence (lanes 1 and 3) or presence 1.6 mM (lane 2 and 4) of Zn^{2+} were probed with specific anti-rTvMP50 polyclonal antibody (at 1:100 dilution) and also probed with anti-α-tubulin (α-TUB) antibody (at 1:100 dilution) as an internal loading control. Arrowheads show the position of native TvMP50 (50 kDa) and α-TUB (55 kDa) proteins. *C*, Zymograms from trichomonad lysates from parasites cultivated in the absence (lanes 1, 2, 5, and 6) or presence of 1.6 mM Zn^{2+} (lanes 3, 4, 7, and 8) from CNCD147 (lanes 1 to 4) and HGMN01 (lanes 5 to 8) *T. vaginalis* isolates that were incubated with cysteine and serine proteinase inhibitors (TLCK, LEUP, E64, and PMSF) (lanes 1 to 8) and with (lanes 2, 4, 6 and 8) or without (1, 3, 5 and 7) metallopeptidase inhibitor (EDTA) for 20 min at 4 °C. Arrows indicate the clear bands of the ~250, ~150, and ~50 kDa protein proteolytic activities. *D*, 2DE zymogram from trichomonad lysate from HGMN01 isolate grown in the presence of Zn^{2+}. Numbers indicate the activity spots. *E*, Analysis of the expression, solubility, purification and proteolytic activity of rTvMP50. SDS-PAGE analysis of the cell extracts before (lane 1) and after (lane 2) IPTG induction, in which a prominent band of 51 kDa is observed (see arrow); soluble (lane 3) and insoluble (lane 4) fractions of rTvMP50 after the disruption of induced cells; and purified rTvMP50 (lane 5; see arrow) after affinity chromatography. The zymograms show the proteolytic activity of purified rTvMP50 (lane 6), which is inhibited in the presence of EDTA (lane 7).

Furthermore, the native TvMP50 was Zn^{2+} differentially expressed in both isolates (Fig. 3*B*). The expression of TvMP50 in the CNCD147 isolate was not observed in the absence of Zn^{2+} (Fig. 3*B*, TvMP50, lane 1), whereas in the presence of Zn^{2+} the band corresponding to native TvMP50 was observed (Fig. 3*B*, TvMP50, lane 2). On the other hand, in the HGMN01 isolate, the native TvMP50 was observed even in the absence of Zn^{2+} (Fig. 3*B*, TvMP50, lane 3) and its expression was increased in the presence of this cation (Fig. 3*B*, TvMP50, lane 4). The expression of α-TUB was not changed by the presence or absence of Zn^{2+} (Fig. 3*B*, α-TUB, lanes 1 to 4).

TvMP50 is a 50-kDa Metalloproteinase—To determine if TvMP50 has proteolytic activity, we generated zymograms using total protein extract obtained from parasites of CNCD147 and HGMN01 isolates grown in the presence or absence of 1.6 mM Zn^{2+} (supplemental Fig. S5 in the Supplemental Data file). As a control, we searched for cysteine proteinase activity and found that the proteolytic activity profiles in reducing conditions in the presence or absence of Zn^{2+} (supplemental Fig. S5 in Supplemental Data file) are in congruence with previous reports (16–17). The proteolytic activity profile under nonreducing conditions was performed at several pH activation values, although the highest proteolytic activity was observed at pH 7.5. The proteolytic activity of proteinases from male and female *T. vaginalis* isolates in nonreducing conditions has not yet been reported. In the CNCD147 isolate, three proteolytic activity bands were observed in the absence (Fig. 3*C* lane 1) or presence of Zn^{2+} (Fig. 3*C*, lane 3). The same proteolytic activity bands were observed in the HGMN01 isolate in the absence (Fig. 3*C* lane 5) or presence of Zn^{2+} (Fig. 3*C*, lane 7). Interestingly, the intensity of the ~50 kDa proteolytic activity band that might correspond to the TvMP50 activity increased in the presence of Zn^{2+} in both isolates.

The inhibition profile of the proteinase extract was tested with zymograms (Fig. 3*C*). Interestingly, the three proteolytic activity bands described above were observed even in the presence of specific cysteine and serine proteinase inhibitors (TLCK, E64, leupeptin, and PMSF) (Fig. 3*C*, lanes 1, 3, 5, and 7), but in the presence of EDTA, a metalloproteinase inhibitor, the activity bands were no longer observed (Fig. 3*C*, lanes 2, 4, 6, and 8), suggesting that the three proteolytic bands, including the 50-kDa band, correspond to the metallopeptidase activity.

In addition, the metallopeptidase activity profile was analyzed with 2DE zymograms. Fig. 3*D* shows a representative zymogram of the metallopeptidase activity profile from the *T. vaginalis* HGMN01. Seven activity spots were detected, three of the spots with a molecular weight (MW) >150 kDa, one of the spots with a MW >50 kDa, two of the spots with a MW of ~50 kDa, and one spot with a MW of ~37 kDa (Fig. 3*D*). Interestingly one of the two spots with a MW of ~50 kDa had a pI of ~5.3, which corresponds to the predicted pI of TvMP50 (5.34).

Furthermore, IPTG-induced *E. coli* harboring the construct pQE80L-*mp50* displayed a band of ~51 KDa (Fig. 3*E*, lane 2), corresponding to rTvMP50, which was not detected in the noninduced control culture (Fig. 3*E*, lane 1). The rTvMP50 was expressed in both the soluble (Fig. 3*E*, lane 3) and insoluble form (Fig. 3*E*, lane 4) and it was purified from the soluble fraction (SF) by nickel affinity chromatography (Fig. 3*E*, lane 5). The protein's identity was confirmed by Western blot analysis using an anti-His Tag antibody (supplemental Fig. S6 in the Supplemental Data file). According to the zymograms, the purified rTvMP50 has proteolytic activity (Fig. 3*E*, lane 6), but it was inhibited in the presence of EDTA (Fig. 3*E*, lane 7).

DISCUSSION

The molecular events during male trichomoniasis remain an area of great interest but are poorly understood. Because iron plays a critical role in host-parasite relationships and in the general physiology of the parasite (26) in the female microenvironment, modulating several pathogenic properties, such as adhesin synthesis (27), protease expression (28), and the expression of crucial metabolic enzymes (26), it seems plausible to infer that in the male microenvironment, Zn^{2+} might has a crucial role as well. Because men are the reservoir of trichomonads, there is an urgent need to identify novel molecular targets for the diagnosis of trichomoniasis in men.

We previously reported that Zn^{2+} has a negative effect on trichomonal cytotoxicity, most likely because of the down-regulation at the protein and transcriptional levels of TvCP65 (16). We also reported at least 27 differentially expressed proteins in the presence of Zn^{2+}in the CNCD147 isolate proteome using 7-cm IPG strips (16). Among these proteins, we found an aminopeptidase P-like metallopeptidase from Clan MG that was up-regulated in the presence of Zn^{2+} (16).

Here, we present a comparative proteomic approach to identify the immunogenic molecules that might be candidates for the development of a male trichomoniasis diagnostic method. To study the influence of the source of the isolate, we used a male (HGMN01) and female (CNCD147) *T. vaginalis* isolate for proteomic analysis. A total of 52 and 29 immunogenic proteins were observed in the HGMN01 and CNCD147 isolates, respectively. Gene Ontology analyses revealed that these immunogenic proteins were involved in diverse biological processes, particularly cytoskeleton organization (20%), glycolysis (7.5%), and carbohydrate metabolism (7.5%).

A proteome reference map of *T. vaginalis* of ~500 protein spots was previously generated with silver-stained 2-DE gels. Although 353 protein spots were excised for MS identification and successfully identified, these spots only represented 64 unique proteins (29). In this study, we excised 52 protein spots that represented 40 unique proteins. The most abundant proteins found in our study were cytoskeleton proteins

and glycolytic proteins. These findings are consistent with the previously mentioned proteome study (29).

The protein profile reported in our study is similar to the protein profile of *T. vaginalis* grown in iron-rich and iron-depleted medium (26). The enzymes involved in energetic metabolism, proteolysis and hydrogenosomal iron-sulfur (Fe-S) proteins were down-regulated or even suppressed in iron-depleted parasites. In contrast, six isoforms of actin, phosphoenolpyruvate carboxykinase, putative lactate dehydrogenase, and putative adenosine triphosphatase were up-regulated (26).

Interestingly, putative cysteine and metallopeptidases were identified as immunogenic molecules. This was not surprising because *T. vaginalis* contains one of the most complex degradomes (more than 400 peptidases) (30) and several molecules from the active degradome are immunogenic (21). *T. vaginalis* expresses several proteinases that participate in many parasitic functions such as trichomonal adherence (31–33), cytotoxicity (17–18, 25, 33), host colonization, hemolysis (34), immune evasion (35–36), signal transduction, nutrient acquisition (34, 37), complement resistant and apoptosis induction (38–39). Moreover, papain-like cysteine proteinases have been described as virulence factors in this parasite (17, 32, 40).

Among the immunogenic proteins, we identified a 50-kDa metallopeptidase of clan MG (TvMP50), which presented an expression level increase of 0.5-fold in the HGMN01 isolate in the presence of Zn^{2+} whereas it was 1.0-fold in the CNCD147 isolate. These data are in agreement with a previous reports (16). Unexpectedly, this metallopeptidase was immunorecognized by the male trichomoniasis patient serum but not by the female patient serum. Although there are many commercial kits for the diagnosis of trichomoniasis, none of them include a specific molecule up-regulated in the male microenvironment. Thus, we propose that TvMP50 might be a promising candidate for male trichomoniasis diagnosis.

The protein and transcript levels of TvMP50 were up-regulated by the presence of Zn^{2+}. This is not the first protease discovered that is up-regulated by the presence of certain cations from the host. For example, Fe^{2+} and polyamines, present in the female microenvironment, down-regulate the protein expression levels and the transcript of TvCP65 (41). In contrast, the amount of mRNA and protein of TvMP50 were up-regulated in the presence of Zn^{2+}.

According to the *T. vaginalis* genome, this parasite contains 13 families of metallopeptidases (30). However, until now, only four metalloproteinases from *T. vaginalis* had been reported (16, 42). Two of them (142 kDa and >220 kDa) were reported by Bozner and Demes, and the activity of these metallopeptidases is inhibited in the presence of 2 mM EDTA (42). Another reported metalloproteinase is a 47-kDa peptidase from the trichomonad hydrogenosome, the hydrogenosomal processing peptidase (HPP). HPP contains an active site motif ($HXXEHX_{76}E$) characteristic of the β subunit of the mitochondrial processing peptidase. Interestingly, HPP forms a homodimer (100 kDa) *in vitro* and *in vivo* (43). The fourth metallopeptidase reported is a 50-kDa proteinase that was up-regulated in the presence of Zn^{2+} in a female *T. vaginalis* isolate (16). However, in the present study, we demonstrate the presence of this metallopeptidase in a male *T. vaginalis* isolate. Interestingly, we found a 50-kDa-proteolytic activity band in the HGMN01 and CNCD147 *T. vaginalis* isolates that might correspond to the previously reported metallopeptidase (16). According to 2DE zymograms, two activity spots of ~50 kDa were observed and the pI of one of the spots corresponded to the predicted pI of TvMP50, suggesting that the proteolytic activity band observed in the one-dimension zymograms corresponds at least to TvMP50. TvMP50 was inhibited by EDTA but not by cysteine or serine proteinase inhibitors such as TLCK, E-64, leupeptin, or PMSF. This proteolytic activity was not detected by Bozner and Demes, possibly because of pH activation. Bozner and Demes activated the proteinases at pH 8.2 (42), whereas we activated them at pH 7.5 because at the basic pH of 8.2, the activity of TvMP50 was not observed. A pH of 7.5 has previously been reported for the activation of metallopeptidases (24). In this study, we performed proteinase activation at several pH values, although the highest proteolytic activity was observed at pH 7.5.

Peptidases with at least two metal ions in the active site are a structurally heterogeneous group. Based on their folds, their active site architectures and the identity of the metal ions, they have been divided into clans MF, MG, and MH in the MEROPS database. Clan MG metallopeptidases, such as the methionine aminopeptidases, have the pita-bread fold and contain two cobalt or two manganese ions in their active centers (44).To identify the residues involved in catalysis, the TvMP50 sequence was aligned with other members of the peptidase clan MG, including aminopeptidase P (Ec_MER001244) and Xaa-Pro dipeptidase (Ec_MER001250) from *Escherichia coli*. The sequence analysis revealed that His215, His324, and His335 are the catalytic residues, whereas Asp232, Asp243, His328, Glu364, and Glu407 are predicted to serve as metal ion ligands in the active site. These results suggest that TvMP50 has an active-site configuration similar to other members of the peptidase clan MG. According to the alignment analyses, TvMP50 might be classified as an aminopeptidase of the clan MG. However, its proteolytic activity and structural characterization remain unknown. A study is currently in progress to elucidate these features.

According to the crystal structures of *E. coli* methionyl aminopeptidase and aminopeptidase P (APP) (45–46), TvMP50 might have diverse metal requirements. The cytosolic and membrane-bound APPs maximum catalytic activities depends on two manganese (Mn^{2+}) or Zn^{2+} ions per subunit, respectively (47). Because TvMP50 was found to be regulated in the presence of Zn^{2+}, we suggest that this molecule might

require this cation for its catalytic activity. Currently, we are determining the metal requirements of TvMP50.

The Role of Some Immunogenic Proteins—To successfully establish infection, pathogenic organisms depend on an arsenal of virulence factors that facilitate host colonization, including adhesins, which are involved in cell binding but also participate in host cell signaling and cellular invasion (48). Five adhesins (AP120, AP65, AP51, AP33, and AP23) were previously reported in *T. vaginalis* (27, 49–53); however, we observed that AP51 was recognized by male trichomoniasis patient serum. Our findings are in agreement with a previous report that demonstrated another molecule involved in adhesion (AP65) was an antigenic protein in *T. vaginalis* (54). Interestingly, AP65 has been used for the diagnosis of trichomoniasis (55).

In general, the expression of surface adhesins and adhesion are iron-dependent phenomena in the female microenvironment (52–53). Despite AP51 being down-regulated by Zn^{2+}, it still unknown how Zn^{2+}directly affects parasite adhesion. A study is in progress to determine the responsible mechanism.

Enolase, a key glycolytic enzyme, is a multifunctional protein that has the ability to serve as a plasminogen receptor on the surface of a variety of hematopoietic, epithelial and endothelial cells. Moreover, α-enolase functions as a heat shock protein (HSP) and binds cytoskeletal and chromatin structures, suggesting a crucial role in transcription and pathophysiological processes (56). When *T. vaginalis* is in contact with vaginal epithelial cells (VECs), the parasite releases α-enolase (tvENO1) but at the same time, it is present on the parasite surface, most likely as an adhesion molecule, suggesting its role as a virulence factor (57). Previously, it had been reported as a *T. vaginalis* enolase family protein (including putative enolase 3 and enolase 4) (58); however, enolase 2 was not included. Although enolase 2 is down-regulated by Zn^{2+}, this molecule was immunorecognized by the male trichomoniasis patient serum in the present study. Furthermore, Whiting and colleagues reported that 15 of 22 patients with proven *Streptococcus pneumoniae* infection have antibodies to α-enolase, suggesting its important role in natural immunity to *S. pneumonia* (59). Elucidating the relationship between antibodies and enolase 2 in male trichomoniasis infection will require further study.

HSPs participate in cellular protection, limiting protein aggregation and facilitating protein folding (60). Moreover, the immunization of BALB/c mice with ΔHSP70-II null mutant promastigotes leads to an effective immune response able to protect these mice against infection with *Leishmania major* (61). Because the Δhsp70-II line could be useful as a platform for introduction of immunoprotective antigens relevant to leishmaniasis (61) or even to other diseases, we propose that the immunogenicity of *T. vaginalis* HSP70 might be used in a trichomoniasis diagnostic method.

Surprisingly, several actin molecules were immunorecognized by the sera of trichomoniasis patients. Identification of a structural protein, such as actin, as an immunogenic molecule has important implications because it is present in all isolates. Although Western blotting analysis revealed that 94% of the IgG-positive sera reacted against *T. vaginalis* α-actinin, also involved in the structure organization (62), the analyzed samples corresponded to infected women. In contrast, our evidence indicated that actin was immunogenic in male trichomoniasis patients. Interestingly, in another study, *Histomonas meleagridis* α-actinin strongly contributed to immune-reaction with hosts, namely turkeys and chickens, and these molecules displayed amino acid identities between 54% and 82.5% (63). The actin genes present in *T. vaginalis* would provide the parasite with a mechanism that allows it to rapidly change its morphology when exposed to different stimuli such as Fe^{2+} or Zn^{2+}. Work is in progress to determine the influence of Zn^{2+}on the morphological appearance of *T. vaginalis*.

Interestingly, we found a C2 domain containing protein as an immunogenic molecule. Moreover, no significant changes in the amount of this protein were found. The C2 domain is a Ca^{2+}-dependent membrane-targeting module found in many cellular proteins involved in signal transduction or membrane trafficking (64).

The energy metabolism of parasites may include the activity of alcohol dehydrogenase, such as *Entamoeba histolytica* in which the pyruvate, the end-product of carbohydrate catabolism by glycolysis, is oxidatively decarboxylated by pyruvate: ferredoxin oxidoreductase (PFOR) (65), transferring the electrons produced during pyruvate oxidation to ferredoxin, whereas acetyl-CoA is consecutively reduced to acetaldehyde and ethanol (under microaerophilic conditions), mainly via the activity of a bifunctional NADH-dependent aldehyde-alcohol dehydrogenase (EhADH2) or to ethanol and acetate (under aerobic conditions) via the latter and acetyl-CoA synthetase (ADP-forming) (65–68). Interestingly, the expression levels of alcohol dehydrogenase 2 (EhADH2) and alcohol dehydrogenase 3 (EhADH3) are higher in a virulent *versus* nonvirulent amoebae (69). Although EhADH3 is present on the plasma membrane surface of *E. histolytica*, the role of EhADH3 in the virulence of amoeba is still unknown (69). On the other hand, EhADH2 is a major adhesion factor only in pathogenic strains and is involved in the internalization of human transfer by *E. histolytica* (70). In *T. vaginalis*, the alcohol dehydrogenase activity is related to metronidazole-resistance. In this case, the trichomonads compensate for the hydrogenosomal deficiency by an increased rate of glycolysis and by changes in their cytosolic pathways (71). *T. vaginalis* enhances lactate fermentation, whereas *T. foetus* activates pyruvate conversion to ethanol. Drug-resistant *T. foetus* also increases activity of the cytosolic NADP-dependent malic enzyme to enhance the pyruvate producing bypass and provide the NADPH required by alcohol dehydrogenase (71). Interestingly, two alcohol dehydrogenases were immunorec-

ognized by the male trichomoniasis patient serum in the present study, but their expression levels did not change in the presence of Zn^{2+}. Because the alcohol acetaldehyde dehydrogenase from *Listeria monocytogenes* (LAP) is a pathogenic factor, promoting bacterial adhesion to intestinal epithelial cells by interacting with mammalian receptor Hsp60 (72–75), it could be possible that this type of enzymes might induce a host immune response.

Currently, the male trichomoniasis diagnosis methods such as APTIMA require a male urethral swab sample (76), which is a painful procedure for the patients. Therefore, the availability of several immunogenic molecules, as shown herein, might facilitate the male immunodiagnosis of *T. vaginalis*.

CONCLUSION

The Zn^{2+} present in the male microenvironment might regulate the expression of several proteins and several of them are immunogenic. The *T. vaginalis* proteome is influenced by the isolate source but also by the presence of Zn^{2+}. The proteome of *T. vaginalis* HGMN01 isolated from a male host consisted of 609 spots, whereas the CNCD147 isolated from a female host consisted of 447. In the presence of Zn^{2+}, 540 spots were found in the HGMN01 isolate and 361 spots were found in the CNCD17 isolate. The male trichomoniasis patient serum recognized 52 and 32 proteins in the HGMN01 or CNCD147 isolate, respectively. These immunogenic proteins are involved in diverse biological processes, particularly cytoskeleton organization, glycolysis, and carbohydrate metabolism.

The 50-kDa metalloproteinase from *T. vaginalis* was differentially expressed in the presence of Zn^{2+} independent of the source of the trichomonads isolate. This molecule was only immunorecognized by the male trichomoniasis patient serum but not by female patient serum, suggesting this molecule as a possible target for the diagnosis of male trichomoniasis.

Acknowledgments—We thank to M. Sc Eduardo Carrillo and Brenda Herrera Villalobos for technical assistance. This work is dedicated to the memory of Dr. Guillermo Mendoza-Hernandez.

* This work was supported by the Universidad Autonoma de la Ciudad de Mexico (UACM) and by grants from ICyTDF (PIFUTP08-150, ICyT 221/2011 and ICyT 18/2012) ICyT 328/2011 and CONACyT (83808) to EAS. LIQG was a scholarship recipient from CONACyT and JLV was supported by ICyTDF.

S This article contains supplemental Tables SI to SVI, Data, Figs. S1 to S6 and Tables S1 to S3.

‖ To whom correspondence should be addressed: Posgrado en Ciencias Genómicas, Universidad Autónoma de la Ciudad de México (UACM), San Lorenzo # 290, Col. Del Valle, CP 03100. México D.F., México. Tel.: (52)5511070280 ext. 15306; Fax: (52)5575-5805; E-mail: elizbethalvarezsanchez@yahoo.com.mx.

REFERENCES

1. WHO, *Global prevalence and incidence of selected curable sexually transmitted infections overview and estimates*, W.H. Organization, Editor. 2001: Geneva. p. 27–29
2. Guenthner, P. C., Secor, W. E., and Dezzutti, C. S. (2005) Trichomonas vaginalis-induced epithelial monolayer disruption and human immunodeficiency virus type 1 (HIV-1) replication: implications for the sexual transmission of HIV-1. *Infect. Immun.* **73,** 4155–4160
3. Schwebke, J. R., and Burgess, D. (2004) *Trichomoniasis. Clin. Microbiol. Rev.* **17,** 794–803
4. El-Shazly, A. M., El-Naggar, H. M., Soliman, M., El-Negeri, M., El-Nemr, H. E., Handousa, A. E., and Morsy, T. A. (2001) A study on *Trichomoniasis vaginalis* and female infertility. *J Egypt Soc. Parasitol.* **31,** 545–553
5. Cotch, M. F., Pastorek II, J. G., Nugent, R. P., and Hillier, S. L. (1997) Trichomonas vaginalis associated with low birth weight and preterm delivery. *Sexually Trans. Dis.* **24,** 353–360
6. Viikki, M., Pukkala, E., Nieminen, P., and Hakama, M. (2000) Gynaecological infections as risk determinants of subsequent cervical neoplasia. *Acta Oncol.* **9,** 71–75
7. Langley, J. G., Goldsmid, J. M., and Davies, N. (1987) Venereal trichomoniasis: role of men. *Genitourin. Med.* **63,** 264–267
8. Sutcliffe, S., Giovannucci, E., Alderete, J. F., Chang, T.-H., Gaydos, C. A., Zenilman, J. M., De Marzo, A. M., Willett, W. C., and Platz, E. A. (2006) Plasma antibodies against *Trichomonas vaginalis* and subsequent risk of prostate cancer. *Cancer Epidemiol. Biomarkers Prevention* **15,** 939–945
9. Sutcliffe, S., Alderete, J. F., Till, C., Goodman, P. J., Hsing, A. W., Zenilman, J. M., De Marzo, A. M., and Platz, E. A. (2009) Trichomonosis and subsequent risk of prostate cancer in the prostate cancer prevention trial. *Int. J. Cancer* **124,** 2082–2087
10. Benchimol, M., de Andrade Rosa, I., da Silva Fontes, R., and Burla Dias, Â. J. (2008) Trichomonas adhere and phagocytose sperm cells: adhesion seems to be a prominent stage during interaction. *Parasitol. Res.* 102, 597–604
11. Krieger, J. N. (1995) Trichomoniasis in men: old issues and new data. *Sexually Trans. Dis.* **22,** 83–96
12. Krieger, J. N., and Rein, M. F. (1982) Zinc sensitivity of *Trichomonas vaginalis*: *in vitro* studies and clinical implications. *J. Infect. Dis.* **146,** 341–345
13. Krieger, J. N., and Rein, M. F. (1982) Canine prostatic secretions kill *Trichomonas vaginalis. Infect. Immun.* **37,** 77–81
14. Fair, W. R., Couch, J., and Wehner, N. (1976) Prostatic antibacterial factor identity and significance. *Urology* **7,** 169–177
15. Gardner, W. A. Jr, Culberson, D. E., and Bennet, B. D. (1986) Trichomonas vaginalis in the prostate gland. *Arch. Pathol. Lab. Med.* **110,** 430–432
16. Vazquez-Carrillo, L. I., Quintas-Granados, L. I., Arroyo, R., Mendoza-Hernández, G., González-Robles, A., Carvajal-Gamez, B. I., and Alvarez-Sánchez, M. E. (2011) The effect of Zn^{2+} on prostatic cell cytotoxicity caused by *Trichomonas vaginalis. J. Integrated Omics* 198–210
17. Alvarez-Sánchez, M. E., Avila-González, L., Becerril-Garcıa, C., Fattel-Facenda, L. V., Ortega-López, J., and Arroyo, R. (2000) A novel cysteine proteinase (CP65) of *Trichomonas vaginalis* involved in cytotoxicity. *Microb. Pathog.* **28,** 193–202
18. Solano-González, E., Alvarez-Sánchez, M. E., Avila-González, L., Rodríguez-Vargas, V. H., Arroyo, R., and Ortega-López, J. (2006) Location of the cell-binding domain of CP65, a 65 kDa cysteine proteinase involved in *Trichomonas vaginalis* cytotoxicity. *Int. J. Biochem. Cell Biol.* **38,** 2114–2127
19. Carvajal-Gamez, B., Arroyo, R., Lira, R., López-Camarillo, C., and Alvarez-Sánchez, M. E. (2010) Identification of two novel *Trichomonas vaginalis* eif-5a genes. *Infect., Genetics and Evol.* **10,** 284–291
20. Leon-Sicairos, C. R., Leon-Felix, J., and Arroyo, R. (2004) tvcp12: a novel *Trichomonas vaginalis* cathepsin L-like cysteine proteinase-encoding gene. *Microbiol.* **150,** 1131–1138
21. Ramon-Luing, L. A., Rendon-Gandarilla, F. J., Cardenas-Guerra, R. E., Rodrıguez-Cabrera, N. A., Ortega-Lopez, J., Avila-Gonzalez, L., Angel-Ortiz, C., Herrera-Sanchez, C. N., Mendoza-Garcıa, M., and Arroyo, R. (2010) Immunoproteomics of the active degradome to identify biomarkers for *Trichomonas vaginalis. Proteomics* **10,** 435–444
22. Hernández-Gutiérrez, R., Avila-González, L., Ortega-López, J., Cruz-Talonia, F., Gómez-Gutierrez, G., and Arroyo, R. (2004) Trichomonas vaginalis: characterization of a 39-kDa cysteine proteinase found in patient vaginal secretions. *Exp. Parasitol.* **107,** 125–135
23. Carvajal-Gamez, B. I., Quintas-Granados, L. I., Arroyo, R., Mendoza-Hernández, G., and Alvarez-Sánchez, M. E. (2012) Translation initiation factor eIF-5A, the hypusine-containing protein, is phosphorylated on serine and tyrosine and O-glycosylated in *Trichomonas vaginalis. Microb.*

Pathog. **52,** 177–183
24. Pucci-Minafra, I., Minafra, S., La Rocca, G., Barranca, M., Fontana, S., Alaimo, G., and Okada, Y. (2001) Zymographic analysis of circulating and tissue forms of colon carcinoma gelatinase A (MMP-2) and B (MMP-9) separated by mono- and two-dimensional electrophoresis. *Matrix Biol.* **20,** 419–427
25. Ramón-Luing, Lde, L., Rendón-Gandarilla, F. J., Puente-Rivera, J., Ávila-González, L., and Arroyo, R. (2011) Identification and characterization of the immunogenic cytotoxic TvCP39 proteinase gene of *Trichomonas vaginalis*. *Int. J. Biochem. Cell Biol.* **43,** 1500–1511
26. De Jesus, J. B., Cuervo, P., Junqueira, M., Britto, C., Silva-Filho, F. C., Soares, M. J., Cupolillo, E., Fernandes, O., and Domont, G. B. (2007) A further proteomic study on the effect of iron in the human pathogen *Trichomonas vaginalis*. *Proteomics* **7,** 1961–1972
27. Moreno-Brito, V., Yáñez-Gómez, C., Meza-Cervantez, P., Ávila-González, L., Rodríguez, M. A., Ortega-López, J., González-Robles, A., and Arroyo, R. (2005) A *Trichomonas vaginalis* 120 kDa protein with identity to hydrogenosome pyruvate:ferredoxin oxidoreductase is a surface adhesin induced by iron. *Cell. Microbiol.* **7,** 245–258
28. Alvarez-Sánchez, M. E., Solano-González, E., Yañez-Gómez, C., and Arroyo, R. (2007) Negative iron regulation of the CP65 cysteine proteinase cytotoxicity in *Trichomonas vaginalis*. *Microbes and Infection* **9,** 1597–1605
29. Huang, K. Y., Chien, K. Y., Lin, Y. C., Hsu, W. M., Fong, I. K., Huang, P. J., Yueh, Y.-M., Gan, R., and Tang, P. (2009) A proteome reference map of *Trichomonas vaginalis*. *Parasitol. Res.* **104,** 927–933
30. Carlton, J. M., Hirt, R. P., Silva, J. C., Delcher, A. L., Schatz, M., Zhao, Q., Wortman, J. R., Bidwell, S. L., Alsmark, U. C. M., Besteiro, S., Sicheritz-Ponten, T., Noel, C. J., Dacks, J. B., Foster, P. G., Simillion, C., Van de Peer, Y., Miranda-Saavedra, D., Barton, G. J., Westrop, G. D., Muller, S., Dessi, D., Fiori, P. L., Ren, Q., Paulsen, I., Zhang, H., Bastida-Corcuera, F. D., Simoes-Barbosa, A., Brown, M. T., Hayes, R. D., Mukherjee, M., Okumura, C. Y., Schneider, R., Smith, A. J., Vanacova, S., Villalvazo, M., Haas, B. J., Pertea, M., Feldblyum, T. V., Utterback, T. R., Shu, C.-L., Osoegawa, K., de Jong, P. J., Hardy, I., Horvathova, L., Zubacova, Z., Dolezal, P., Malik, S.-B., Logsdon, K. M. J., Henze, K., Gupta, A., Wang, C. C., Dunne, R. L., Upcroft, J. A., Upcroft, P., White, O., Salzberg, S. L., Tang, P., Chiu, C.-H., Lee, Y.-S., Embley, T. M., Coombs, G. H., Mottram, J. C., Tachezy, J., Fraser-Liggett, C. M., and Johnson, P. J. (2007) Draft genome sequence of the sexually transmitted pathogen *Trichomonas vaginalis*. *Science* **31,** 207–212
31. Arroyo, R., and Alderete, J. F. (1989) Trichomonas vaginalis surface proteinase activity is necessary for parasite adherence to epithelial cells. *Infect. Immun.* **57,** 2991–2997
32. Mendoza-Lopez, M. R., Becerril-Garcia, C., Fattel-Facenda, L. V., Avila-Gonzalez, L., Ruiz-Tachiquin, M. E., Ortega-Lopez, J., and Arroyo, R. (2000) CP30, a cysteine proteinase involved in *Trichomonas vaginalis* cytoadherence. *Infect. Immun.* **6,** 4907–4912
33. Hernández, H., Sariego, I., Garber, G., Delgado, R., López, O., and Sarracent, J. (2004) Monoclonal antibodies against a 62 kDa proteinase of *Trichomonas vaginalis* decrease parasite cytoadherence to epithelial cells and confer protection in mice. *Parasite Immunol.* **26,** 119–125
34. Dailey, D. C., Chang, T. H., and Alderete, J. F. (1990) Characterization of *Trichomonas vaginalis* haemolysis. *Parasitol.* **101,** 171–175
35. Alderete, J. F., Provenzano, D., and Lehker, M. W. (1995) Iron mediates *Trichomonas vaginalis* resistance to complement lysis. *Microb. Pathog.* **19,** 93–103
36. Provenzano, D., and Alderete, J. F. (1995) Analysis of human immunoglobulin-degrading cysteine proteinase of *Trichomonas vaginalis*. *Infect. Immun.* **63,** 3388–3395
37. Lehker, M. W., Chang, T. H., Dailey, D. C., and Alderete, J. F. (1990) Specific erythrocyte binding is an additional nutrient acquisition system for *Trichomonas vaginalis*. *J. Exp. Med.* **171**,
38. Sommer, U., Costello, C. E., Hayes, G. R., Beach, D. H., Gilbert, R. O., Lucas, J. J., and Singh, B. N. (2005) Identification of *Trichomonas vaginalis* cysteine proteases that induce apoptosis in human vaginal epithelial cells. *J. Biol. Chem.* **280,** 23853–23860
39. Kummer, S., Hayes, G. R., Gilbert, R. O., Beach, D. H., Lucas, J. J., and Singh, B. N. (2008) Induction of human host cell apoptosis by *Trichomonas vaginalis* cysteine proteases is modulated by parasite exposure to iron. *Microb. Pathog.* **44,** 197–203
40. Hernandez-Gutierrez, R., Ortega-López, J., and Arroyo, R. (2003) A 39-kDa cysteine proteinase CP39 from *Trichomonas vaginalis*, which is negatively affected by iron may be involved in trichomonal cytotoxicity. *J. Euk. Microbiol.* **50,** 696–698
41. Alvarez-Sanchez, M. E., Carvajal-Gamez, B. I., Solano-Gonzalez, E., Martinez-Benitez, M., Garcia, A. F., Alderete, J. F., and Arroyo, R. (2008) Polyamine depletion down-regulates expression of the *Trichomonas vaginalis* cytotoxic CP65, a 65-kDa cysteine proteinase involved in cellular damage. *J. Biochem. Cell Biol.* **40,** 2442–2451
42. Bozner, P., and Demes, P. (1990) Proteinases in *Trichomonas vaginalis* and *Tritrichomonas mobilensis* are not exclusively of cysteine type. *Parasitol.* **102**, 113–115
43. Brown, M. T., Goldstone, H. M., Bastida-Corcuera, F., Delgadillo-Correa, M. G., McArthur, A. G., and Johnson, P. J. (2007) A functionally divergent hydrogenosomal peptidase with protomitochondrial ancestry. *Mol. Microbiol.* **64,** 1154–1163
44. Bazan, J. F., Weaver, L. H., Roderick, S. L., Huber, R., and Matthews, B. W. (1994) Sequence and structure comparison suggest that methionine aminopeptidase, prolidase, aminopeptidase P, and creatinase share a common fold. *Proc. Natl. Acad. Sci. U.S.A.* **91,** 2473–2477
45. Wilce, M. C., Bond, C. S., Dixon, N. E., Freeman, H. C., Guss, J. M., Lilley, P. E., and Wilce, J. A. (1998) Structure and mechanism of a proline-specific aminopeptidase from *Escherichia coli*. *Proc. Natl. Acad. Sci. U.S.A.* **95,** 3472–3477
46. Roderick, S. L., and Matthews, B. W. (1993) Structure of the cobalt-dependent methionine aminopeptidase from *Escherichia coli*: a new type of proteolytic enzyme. *Biochemistry* **32,** 3907–3912
47. Cottrell, G. S., Hooper, N. M., and Turner, A. J. (2000) Cloning, expression, and characterization of human cytosolic aminopeptidase P: A single manganese(II)-dependent enzyme. *Biochemistry* **39,** 15121–15128
48. Konto-Ghiorghi, Y., Mairey, E., Mallet, A., Duménil, G., Caliot, E., Trieu-Cuot, P., and Dramsi, S. (2009) Dual role for pilus in adherence to epithelial cells and biofilm formation in *Streptococcus agalactiae*. *PLoS Pathog.* **5**, e1000422
49. Ardalan, S., Lee, B. C., and Garber, G. E. (2009) Trichomonas vaginalis: The adhesins AP51 and AP65 bind heme and hemoglobin. *Exp. Parasitol.* **121,** 300–306
50. Arroyo, R., Engbring, J., and Alderete, J. F. (1992) Molecular basis of host epithelial cell recognition by *Trichomonas vaginalis*. *Mol. Microbiol.* **6,** 853–862
51. Arroyo, R., and Alderete, J. F. (1995) Trichomonas vaginalis surface proteinases bind to host epithelial cells and are related to levels of cytoadherence and cytotoxicity. *Arch. Med. Res.* **26,** 279–285
52. Garcia, A. F., Chang, T. H., Benchimol, M., Klumpp, D. J., Lehker, M. W., and Alderete, J. F. (2003) Iron and contact with host cells induce expression of adhesins on surface of *Trichomonas vaginalis*. *Mol. Microbiol.* **47,** 1207–1224
53. Lehker, M. W., Arroyo, R., and Alderete, J. F. (1991) The regulation by iron of the synthesis of adhesins and cytoadherence levels in the protozoan *Trichomonas vaginalis*. *J. Exp. Med.* **174,** 311–318
54. Lee, H. Y., Hyung, S., Lee, J. W., Kim, J., Shin, M. H., Ryu, J.-S., and Park, S. J. (2011) Identification of antigenic proteins in *Trichomonas vaginalis*. *Korean J. Parasitol.* **49,** 79–83
55. Alderete, J. F., Nguyen, J., Mundodi, V., and Lehker, M. W. (2004) Heme-iron increases levels of AP65-mediated adherence by *Trichomonas vaginalis*. *Microb. Pathog.* **36,** 263–271
56. Pancholi, V. (2001) Multifunctional α-enolase: its role in diseases. *Cell. Mol. Life Sciences* **58,** 902–920
57. Mundodi, V., Kucknoor, A. S., and Alderete, J. F. (2008) Immunogenic and plasminogen-binding surface-associated α-enolase of *Trichomonas vaginalis*. *Infection Immunity* **76,** 523–531
58. De Jesus, J. B., Cuervo, P., Junqueira, M., Britto, C., Costa Silva-Filho, F., Saboia-Vahia, L., Gonzalez, L. J., and Barbosa Domont, G. (2007) Application of two-dimensional electrophoresis and matrix-assisted laser desorption/ionization time-of-flight mass spectrometry for proteomic analysis of the sexually transmitted parasite *Trichomonas vaginalis*. *J. Mass Spectrometry* **42,** 1463–1473
59. Whiting, G. C., Evans, J. T., Patel, S., and Gillespie, S. H. (2002) Purification of native α-enolase from *Streptococcus pneumoniae* that binds plasminogen and is immunogenic. *J. Med. Microbiol.* **51,** 837–843
60. Kim, H. P., Morse, D., and Choi, A. M. (2006) Heat-shock proteins: new

keys to the development of cytoprotective therapies. *Expert. Opin. Ther. Targets.* **10,** 759–769
61. Carrion, J., Folgueira, C., Soto, M., Fresno, M., and Requena, J. (2011) Leishmania infantum HSP70-II null mutant as candidate vaccine against leishmaniasis: a preliminary evaluation. *Parasites & Vectors* **4,** 150
62. Addis, M. F., Rappelli, P., Pinto de Andrade, A. M., Rita, F. M., Colombo, M. M., Cappuccinelli, P., and Fiori, P. L. (1999) Identification of *Trichomonas vaginalis* α-actinin as the most common immunogen recognized by sera of women exposed to the parasite. *J. Infect. Dis.* **180,** 1727–1730
63. Leberl, M., Hess, M., and Bilic, I. (2010) Histomonas meleagridis possesses three α-actinins immunogenic to its hosts. *Mol. Biochem. Parasitol.* **169,** 101–107
64. Yasunaga, S., Grati, M., Cohen-Salmon, M., El-Amraoui, A., Mustapha, M., Salem, N., El-Zir, E., Loiselet, J., and Petit, C. (1999) A mutation in OTOF, encoding otoferlin, a FER-1-like protein, causes DFNB9, a nonsyndromic form of deafness. *Nat. Genet.* **21,** 363–369
65. Reeves, R. E., Warren, L. G., Susskind, B., and Lo, H. S. (1977) An energy conserving pyruvate-to-acetate pathway in *Entamoeba histolytica. J. Biol. Chem.* **257,** 726–731
66. Pineda, E., Encalada, R., Rodríguez-Zavala, J. S., Olivos-García, A., Moreno-Sánchez, R., and Saavedra, E. (2010) Pyruvate:ferredoxin oxidoreductase and bifunctional aldehyde–alcohol dehydrogenase are essential for energy metabolism under oxidative stress in *Entamoeba histolytica. FEBS J.* **277,** 3382–3395
67. Reeves, R. E. (1984) Metabolism of *Entamoeba histolytica. Adv. Parasitol.* **23,** 105–142
68. Lo, H. S., and Reeves, R. E. (1978) Pyruvate-to-ethanol pathway in *Entamoeba histolytica. Biochem. J.* **171,** 225–230
69. Davis, P. H., Chen, M., Zhang, X., Clark, C. G., Townsend, R. R., and Stanley, S. L., Jr. (2009) Proteomic comparison of *Entamoeba histolytica* and *Entamoeba dispar* and the role of *E. histolytica* alcohol dehydrogenase 3 in virulence. *PLoS Negl. Trop. Dis.* **3,** e415
70. Reyes-López, M., Bermúdez-Cruz, R. M., Avila, E. E., and de la Garza, M. (2011) Acetaldehyde/alcohol dehydrogenase-2 (EhADH2) and clathrin are involved in internalization of human transferrin by *Entamoeba histolytica. Microbiology* **157,** 209–219
71. Jaroslav, K. (1999) Trichomonads, hydrogenosomes and drug resistance. *Int. J. Parasitol.* **29,** 199–212
72. Jagadeesan, B., Koo, O. K., Kim, K.-P., Burkholder, K. M., Mishra, K. K., Aroonnual, A., and Bhunia, A. K. (2010) LAP, an alcohol acetaldehyde dehydrogenase enzyme in *Listeria*, promotes bacterial adhesion to enterocyte-like Caco-2 cells only in pathogenic species. *Microbiology* **156,** 2782–2795
73. Jaradat, Z. W., Wampler, J. W., and Bhunia, A. W. (2003) A *Listeria* adhesion protein-deficient *Listeria monocytogenes* strain shows reduced adhesion primarily to intestinal cell lines. *Med. Microbiol. Immunol.* **192,** 85–91
74. Pandiripally, V. K., Westbrook, D. G., Sunki, G. R., and Bhunia, A. K. (1999) Surface protein p104 is involved in adhesion of *Listeria monocytogenes* to human intestinal cell line, Caco-2. *J. Med. Microbiol.* **48,** 117–124
75. Wampler, J. L., Kim, K. P., Jaradat, Z., and Bhunia, A. K. (2004) Heat shock protein 60 acts as a receptor for the *Listeria* adhesion protein in Caco-2 cells. *Infect. Immun.* **72,** 931–936
76. Nye, M. B., Schwebke, J. R., and Body, B. A. (2009) Comparison of APTIMA *Trichomonas vaginalis* transcription-mediated amplification to wet mount microscopy, culture, and polymerase chain reaction for diagnosis of trichomoniasis in men and women. *Am. J. Obstet. Gynecol.* **200,** 1–7